Effect of Different Diesel Fuels on Formation of the Cavitation Phenomena

Mohammadreza Nezamirad, Sepideh Amirahmadian, Nasim Sabetpour, Azadeh Yazdi, Amirmasoud Hamedi

***Abstract*—**Cavitation inside a diesel injector nozzle is investigated numerically in this study. The Reynolds Stress Navier Stokes set of equations (RANS) are utilized to investigate flow behavior inside the nozzle numerically. Moreover, K-ε turbulent model is found to be a better approach comparing to K-ω turbulent model. The Winklhofer rectangular shape nozzle is also simulated in order to verify the current numerical scheme, and with the mass flow rate approach, the current solution is verified. Afterward, a six-hole real size nozzle was simulated and it was found that among the different fuels used in this study with the same condition, diesel fuel provides the largest length of cavitation. Also, it was found that at the same boundary condition, rapeseed methyl ester (RME) fuel leads to the highest value of discharge coefficient and mass flow rate.

***Keywords*—**Cavitation, diesel fuel, CFD, real size nozzle, discharge coefficient.

I. Introduction

CAVITATION in modern combustion engines is of interest and can affect the efficiency of the combustion process significantly. Cavitation occurs when the pressure drops noticeably, and the liquid turns to vapor, which are shown as vapor volume fraction in most of the studies [1]-[3]. There are two different phenomena that can cause vapor formation: the first one is boiling, that occurs due to temperature increment, and the second one is cavitation that happens due to sudden pressure drop. There are occasions in which both increasing temperature and decreasing pressure occur simultaneously, which is not in the scope of the current study. There are two approaches for modeling cavitating flow depending on the problem of interest, which are the Euler-Euler approach and the Euler-Lagrange approach [4], [5].

By utilizing the Eulerian-Eulerian approach, which is so called two-fluid approach, each phase using its own corresponding velocity is solved for both phases [6], [7]. The predominant hypothesis in the mentioned models is thermal equilibrium in which it assumes that phase change is very rapid and achieving thermal equilibrium is much quicker when the time interval is utilized [8]-[11]. The second approach is Eulerian-Lagrangian, in which two different couplings can be used that are one-way coupling and two-way coupling. Within one-way coupling, Eulerian solution is obtained first and then will feed the Lagrangian solution, while in the two-way coupling there is an interactive relationship between Eulerian phase and Lagrangian phase [12]-[14].

One of the first experimental studies that was done in diesel injector cavitation was by Winklhofer et al. [15]. He reported static pressure, velocity field and vapor fraction inside the channel. Then, the mentioned study is used afterward in many literatures for verification purposes.

II. Mathematical Model

In this study, two phase flow is simulated based on single fluid approach for homogenous framework. The continuous and momentum equations for homogenous flow can be written as follows:

$$\frac{\partial}{\partial t}(\rho_m) + \nabla.(\rho_m \vec{v}_m) = 0 \quad (1)$$

$$\frac{\partial}{\partial t}(\rho_m) + \nabla.(\rho_m \vec{v}_m.\vec{v}_m) = -\nabla p + \nabla.[\mu_m(\nabla\vec{v}_m + \nabla\vec{v}_m^T)] + \rho_m\vec{g} \quad (2)$$

in which ρ_m is mixture density, $\vec{v}_m$ is the mixture velocity vector and μ_m is the mixture viscosity, where mixture density can be written as $\rho_m=\alpha_l\rho_l+\alpha_v\rho_v$ and mixture viscosity can be written as $\mu_m=\alpha_l\mu_l+\alpha_v\rho_v$.

Vapor volume fraction is a criterion in which it determines the estimate of vapor presence versus liquid and can be shown as follows:

$$\alpha_v = \frac{n_b \frac{4}{3}\pi R_B^3}{1+n_b \frac{4}{3}\pi R_B^3} \quad (3)$$

where α_v is the vapor volume fraction, n_b is number of bubbles per unit volume and R_B is the bubble radius.

In order to obtain mass transfer, Shnerr-Sauer model is utilized [14]:

$$\frac{\partial}{\partial t}(\alpha_v.\rho_v) + \nabla.(\alpha_v.\rho_v.V_v) = \frac{\rho_v.\rho_l}{\rho}.\frac{d\alpha_v}{dt} \quad (4)$$

in which the source term is define as $R=\frac{\rho_v\rho_l}{\rho}\frac{d\alpha_v}{dt}$. Bubble radius is also defined as $R_B=(\frac{\alpha_v}{1-\alpha_v}\frac{3}{4\pi}\frac{1}{n_b})^{\frac{1}{3}}$.

Discharge coefficient and cavitation number are the two important parameters that are respectively defined as following:

$$Cd = \frac{\dot{m}}{A\sqrt{2\rho_l(P_{in}-P_{back})}} \quad (5)$$

$$K = \frac{P_{in}-P_v}{P_{in}-P_{back}} \quad (6)$$

Mohammadreza Nezamirad is with the University of South Florida, USA (e-mail: mnezamirad@usf.edu).

where $\dot{m}$ is mass flow rate, P_v is vaporization pressure, P_{in} is inlet pressure and P_{back} is the outlet pressure.

A. Verification

In the beginning, the flow is verified by comparing to a previous experiment that was done by Winklhofer et al. [15]. Fig. 1 shows mass flow rate versus pressure difference when two different turbulent approaches are utilized, namely $K-\varepsilon$ and $K-\omega$. When compared to experimental data, it was found that $K-\varepsilon$ has better accuracy. It was also found that as pressure difference increases, mass flow rate increases as well until it does not change anymore.

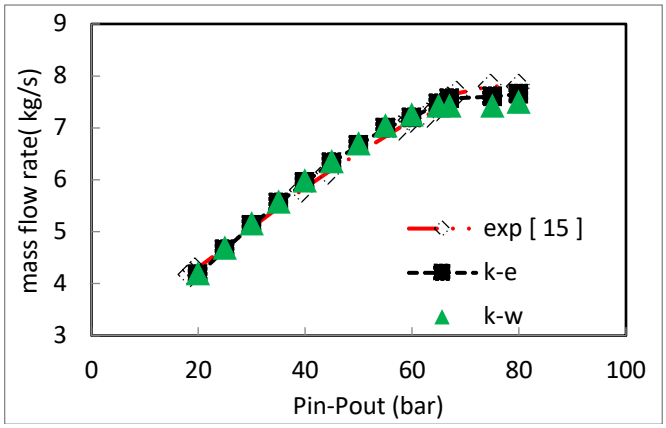

Fig. 1 Mass flow rate versus pressure

III. Real-Size Nozzle

Fig. 2 shows the geometry of the real size nozzle. It can be seen that the inlet radius is 13 mm, the maximum needle height is 250 μm, orifice diameter is 170 μm and orifice length is 970 μm. Also, in order to save time and resources, only one-sixth of the nozzle is simulated by the acquisition of periodic boundary conditions.

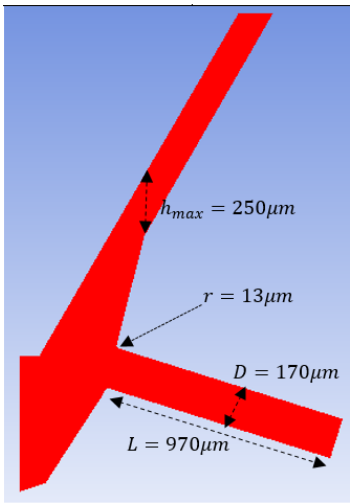

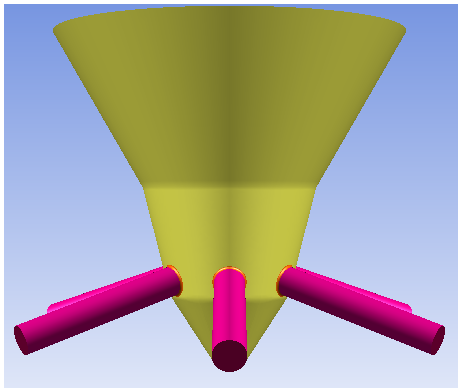

Fig. 2 Geometry of the real size nozzle

Table I shows the properties of the fuels utilized in this study. Diesel fuel has the lowest value of density among all three fuels, while Rapeseed pure vegetable oil (R-PVO) has the highest value. The property of rapeseed methyl ester (RME) is between R-PVO and Diesel fuel.

TABLE I
PROPERTIES OF FUELS USED IN THIS STUDY

	Diesel fuel	RME[1] fuel	R-PVO[2] fuel
Density (kg/m^3)	830	880	890
Dynamic viscosity (Ns/m^2)	3.61×10^3	4.62×10^3	6.31×10^3
Vaporization pressure (Pa)	890	923	996
Temperature (K)	293	293	293
Number of bubbles per unit volume	$10^{11} \times 1.9$	$10^{11} \times .91$	$10^{11} \times .91$

IV. Result and Discussion

Fig. 3 shows the mass flow rate versus pressure difference when different fuels are utilized. As can be seen from Fig. 3, increasing pressure difference increases mass flow to a certain value, and after that, any further increase would not change the mass flow rate. The highest value of mass flow rate is seen in both RME and R-PVO fuel, while the lowest value is observed for diesel fuel. In all three fuels at maximum needle height, increasing pressure difference has the same trend, but for RME, the case is a little bit different, and a decreasing trend is

visualized after it reached a certain value. The increase in the value of the mass flow rate by pressure increase was very steep for R-PVO compared to the other two fuels.

Fig. 4 shows the discharge coefficient versus cavitation number at the maximum needle height when three different fuels are utilized. According to Fig. 4, increasing the cavitation number would increase the discharge coefficient to a certain value, and after that, a further increase in the cavitation number would not increase the discharge coefficient, and it remains constant. The highest value of the discharge coefficient is visualized for RME fuel, while the lowest value is observed for diesel fuel. It can be concluded that even though the mass flow rate can show a similar trend with the discharge coefficient, other factors can play a crucial role; since the difference in the discharge coefficient of RME and R-PVO when the cavitation number increases at the maximum needle height are noticeable, while the difference between the mass flow rate of RME and R-PVO as the pressure difference increases is not very bold.

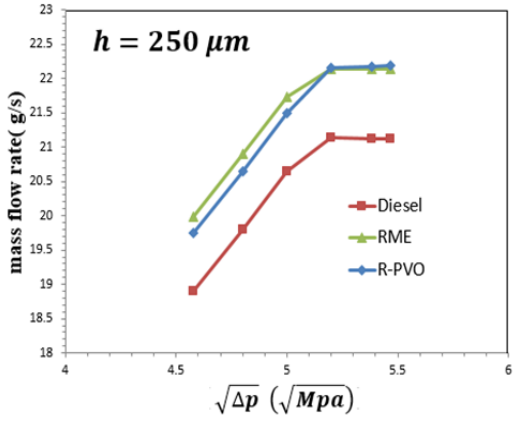

Fig. 3 Mass flow rate versus pressure difference when three different fuels are used

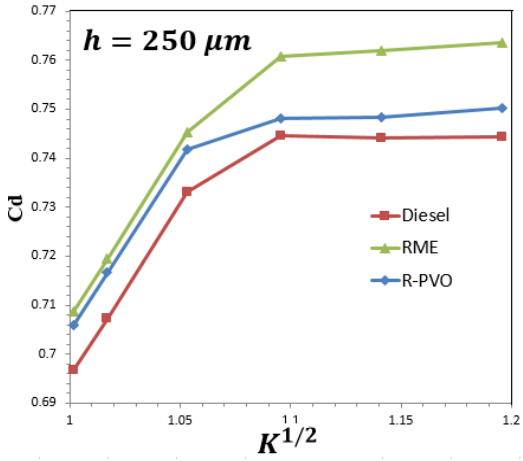

Fig. 4 Discharge coefficient versus cavitation number when different fuels are utilized

Fig. 5 shows the distribution of the vapor volume fraction when the needle height has its maximum value, the pressure inlet is 30 MPa, and the pressure outlet is 3 MPa. It can be seen that R-PVO has the shortest distribution of vapor volume fraction through the nozzle, while diesel fuel has the largest distribution of vapor volume fraction through the nozzle. The primary and key factor for the mentioned behavior of vapor volume fraction is viscosity as the highest value of viscosity is for R-PVO fuel, and the lowest value of viscosity is for diesel fuel.

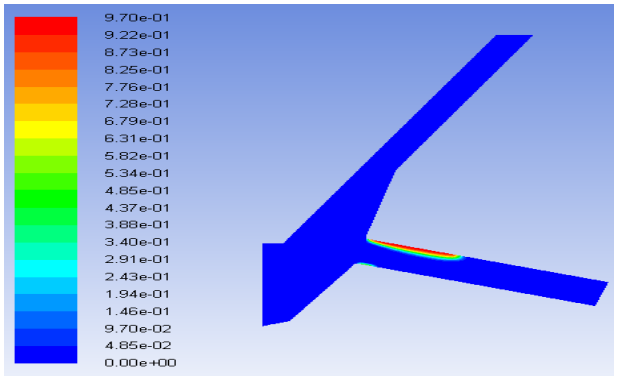

(a) R-PVO fuel

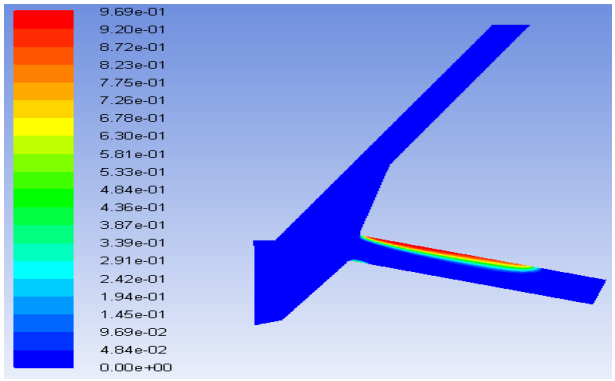

(b) RME fuel

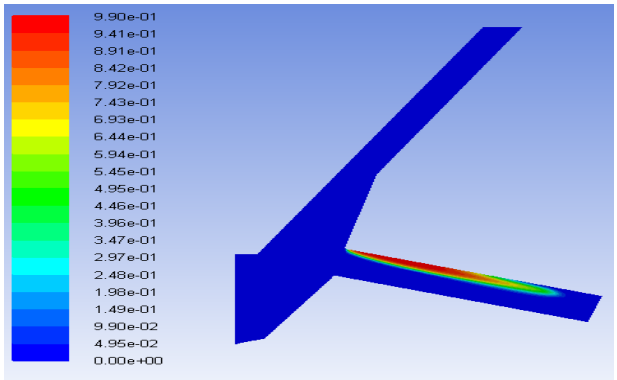

(c) Diesel fuel

Fig. 5 Vapor volume fraction distribution at the mid nozzle plane when three different fuels are utilized

Figure 6 shows the distribution of vapor volume fraction when different back pressures are utilized. As the mentioned figure represents, by increasing backpressure when the inlet pressure is fixed, the length of vapor volume fraction increases. The inlet pressure is fixed to 30 Mpa, and the outlet pressure varies. Also, the needle height is 250 μm. It was also found that further decrease in the back pressure from 1 MPa would not affect the

formation of vapor volume fraction.

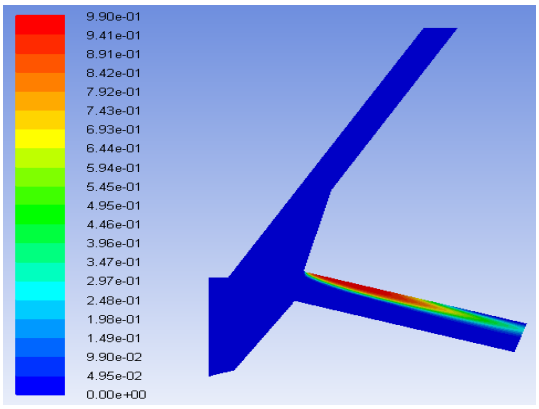

(a) $P_{back} = 1Mpa$

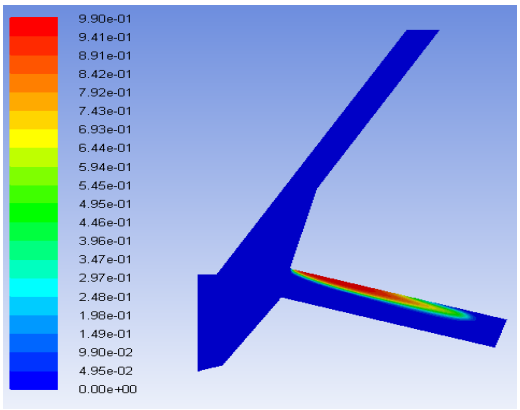

(b) $P_{back} = 3Mpa$

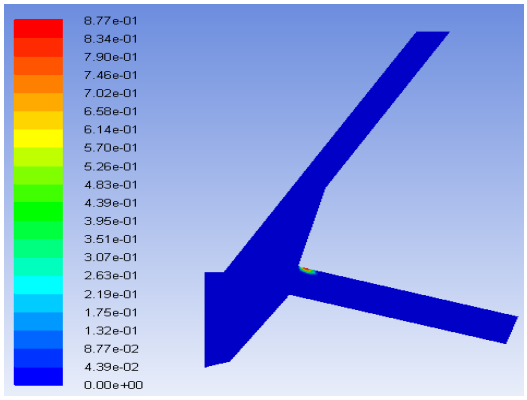

(c) $P_{back} = 5Mpa$

Fig. 6 Vapor volume fraction distribution at the mid nozzle plane when three different back pressures

Effect of needle height on the formation of vapor volume fraction has also been investigated. As figure 7 shows, by increasing the needle height, the length of the cavitation area increases. When needle height was h=30µm, cavitation formed out of the orifice area in the needle region. While as needle height increases, the length of the vapor volume fraction is augmented. And finally, at h=250µm, cavitation covered the whole orifice.

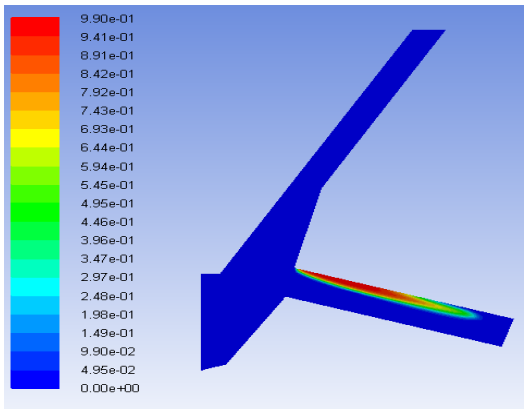

(a) $h = 250\mu m$

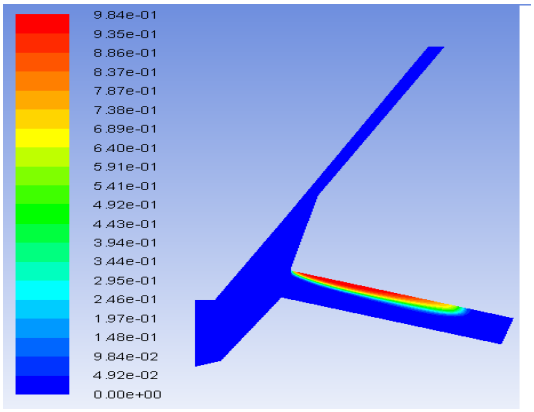

(b) $h = 100\mu m$

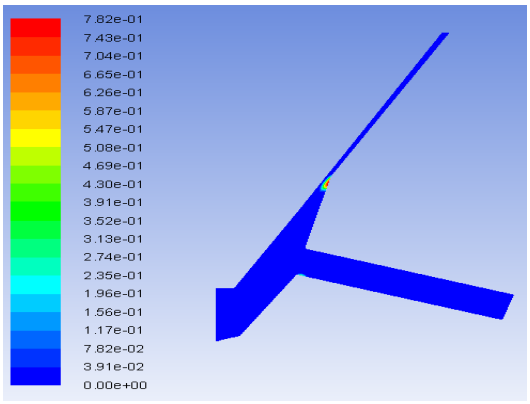

(c)$h = 30\mu m$

Fig. 7 Vapor volume fraction distribution at the mid nozzle plane when three different needle height

V. Conclusion

In this study, a six-hole nozzle is simulated in order to investigate the effect of different fuels on the formation of vapor volume fraction, the value of discharge coefficient, and mass flow rate. The results were also verified with previous experimental data obtained by Winklhofer et al. [15] in terms of mass flow. The Schnerr-Sauer cavitation model is also utilized to predict cavitation inside the nozzle. It was found that at the same condition, diesel fuel has the largest length of vapor volume fraction, while R-PVO fuel has the smallest length.

RME fuel also has the highest value of discharge coefficient as the cavitation number increases at maximum needle height, while diesel fuel has the lowest value. Mass flow rates for both RME and R-PVO experience the same trend and are much higher than diesel fuel as pressure difference increases. Also, it was found that increasing needle height would increase the length of vapor volume fraction, which means that cavitation length increases. Finally, decreasing backpressure would increase the length of the cavitation area. A further decrease from 1 Mpa in the backpressure would not affect cavitation formation significantly.

REFERENCES

[1] Zeidi, S. and M. Mahdi, Investigation the effects of injection pressure and compressibility and nozzle entry in diesel injector nozzle's flow. Journal of Applied and Computational Mechanics, 2015. 1(2): p. 83-94.
[2] Zeidi, S. and M. Mahdi. Investigation of viscosity effect on velocity profile and cavitation formation in Diesel injector nozzle. in Proceedings of the 8th international conference on internal combustion engines. 2014.
[3] Zeidi, S. M. J. and M. Mahdi, Evaluation of the physical forces exerted on a spherical bubble inside the nozzle in a cavitating flow with an Eulerian/Lagrangian approach. European Journal of Physics, 2015. 36(6).
[4] Giannadakis, E., M. Gavaises, and C. Arcoumanis, Modelling of cavitation in diesel injector nozzles. Journal of Fluid Mechanics, 2008. 616: p. 153-193.
[5] Farrell, K. J., Eulerian/Lagrangian analysis for the prediction of cavitation inception. Journal of Fluids Engineering-Transactions of the Asme, 2003. 125(1): p. 46-52.
[6] Ma, J. S., G. L. Chahine, and C.T. Hsiao, Spherical bubble dynamics in a bubbly medium using an Euler-Lagrange model. Chemical Engineering Science, 2015. 128: p. 64-81.
[7] Maeda, K. and T. Colonius, A source term approach for generation of one-way acoustic waves in the Euler and Navier-Stokes equations. Wave Motion, 2017. 75: p. 36-49.
[8] Peters, A., U. Lantermann, and O. el Moctar, Simulation of an Internal Nozzle Flow Using an Euler-Lagrange Method, in Proceedings of the 10th International Symposium on Cavitation (CAV2018), J. Katz, Editor. 2018, ASME Press. p. 0.
[9] Ellahi, R., et al., Simulation of cavitation of spherically shaped hydrogen bubbles through a tube nozzle with stenosis. International Journal of Numerical Methods for Heat & Fluid Flow, 2020. 30(5): p. 2535-2549.
[10] Wang, Y. -C. and C. Brennen, Shock waves and noise in the collapse of a cloud of cavitation bubbles. 1995.
[11] Hsiao, C. T., G. L. Chahine, and H. L. Liu, Scaling effect on prediction of cavitation inception in a line vortex flow. Journal of Fluids Engineering-Transactions of the Asme, 2003. 125(1): p. 53-60.
[12] Pearce, D., Pressure waves and cavitation in diesel fuel injection rate characterisation. 2017, Imperial College London.
[13] Fu, Y., Z. P. Xie, and W. G. Zhao, Prediction Method of Cavitation Jet Wave Attenuation Based on Five-Equation Two-Fluid Model. Mathematical Problems in Engineering, 2020. 2020.
[14] Schnerr, G. H. and J. Sauer. Physical and numerical modeling of unsteady cavitation dynamics. in Fourth international conference on multiphase flow. 2001. ICMF New Orleans.
[15] Winklhofer, E., et al. Comprehensive hydraulic and flow field documentation in model throttle experiments under cavitation conditions. in Proceedings of the ILASS-Europe conference, Zurich. 2001.